RSC Advances

ROYAL SOCIETY OF CHEMISTRY

www.rsc.org/advances

RSC Advances

RSCPublishing

ARTICLE

Metallicity Enhancement in Core-shell SiO_2@RuO_2 Nanowires

Cite this: DOI: 10.1039/x0xx00000x

J. I. Martínez,*[a] F. Calle-Vallejo,[b] E. Abad[c] and J. A. Alonso[d]

Received 00th January 2014,
Accepted 00th January 2014

DOI: 10.1039/x0xx00000x

www.rsc.org/

Metallic oxide compounds have interesting applications in catalysis, in optoelectronics, and as sensitive detectors. One of these, RuO_2, is also an excellent material for charge storage. Composite core–shell nanowires formed by an inner insulating SiO_2 wire serving as scaffold to an external RuO_2 nanotube have promising uses. Electronic structure calculations reveal an interesting modification of the electronic band structure of the external oxide shell induced by the presence of the SiO_2 core. The small changes in the interatomic distances in RuO_2 as it adapts to the underlying core lead to some bands crossing the Fermi level, and to an enhancement in the metallicity of the system. As a consequence, a substantial increase of the conductance of the wires is predicted when the composite SiO_2@RuO_2 wires are accommodated between two gold electrodes. The result suggests that the small strain occurring as metal-oxide wires adapt to the insulating core can be used to tailor the electrical conductance.

Metallic oxide compounds have attracted increasing attention due to their wide applicability range as catalysts,[1–4] in optoelectronics,[5,6] and as highly sensitive detectors,[7] to name just a few. Additionally, a large variety of metallic oxides exhibits enhanced paramagnetic, ferromagnetic, and antiferromagnetic behaviors, which can be combined in layered heterojunctions.[8] The study of nanostructured metallic oxides, such as monolayers, surfaces, nanoclusters and nanotubes,[9,10] has arisen as an area with promising technological applications. It is important to notice the advances in the study of their electronic, magnetic and optical properties, which can be tuned, depending on the targeted functionality, by introducing structural defects or just by doping. As a consequence, the step from laboratory research towards design and fabrication of devices is nowadays getting closer.

A paradigmatic example of metallic oxide compound is ruthenia, RuO_2, which has a low resistance and high thermal and chemical stabilities at ambient conditions, yielding a good material for applications such as corrosion-resistant electrodes for chlorine or oxygen evolution,[11,12] or as a catalytic agent for photodissociation of water.[13] Ruthenia is an extraordinary material for charge storage[14] that possesses the highest measured efficiency. Employing cores of an inexpensive material acting as its scaffolding becomes an ideal way to reduce the content of the expensive metal ruthenium. Following this line, cylindrical fibers and nanowires have been synthesized formed by a thin RuO_2 shell surrounding the inner solid core formed by a SiO_2 nanowire.[15] This has motivated us to study small diameter composite SiO_2@RuO_2 nanowires with the purpose of assessing their electronic and conducting properties. Most low diameter SiO_2 nanowires have semiconducting character.[16] The constraints imposed on the surrounding RuO_2 shell by the underlying core may somehow affect its structure and electronic properties (as compared to the properties of empty RuO_2 nanotubes[10]). Indeed, we find that the electronic structure of the RuO_2 shell suffers changes in the region near the Fermi energy, which lead to a substantial enhancement of the conductance. This finding suggests a new method to modify the electronic and conducting properties of metal-oxide nanowires and nanotubes, by preparing a core-shell nanocomposite wire with the thin metal oxide shell surrounding an inner SiO_2 core.

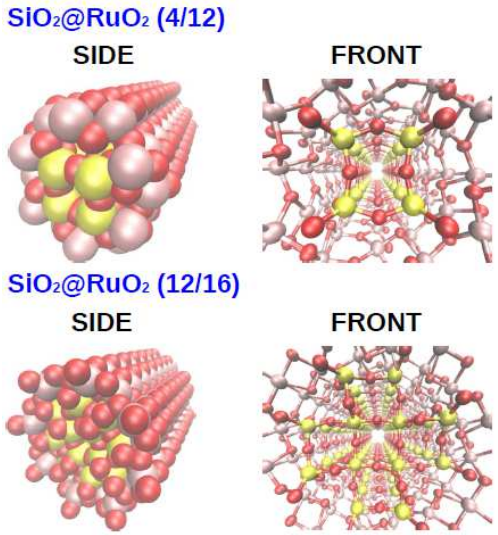

Figure 1. Side and front views of the two optimized SiO_2@RuO_2 nanowire models used in the present study. O, Si and Ru atoms are represented by red, yellow and pink spheres, respectively.

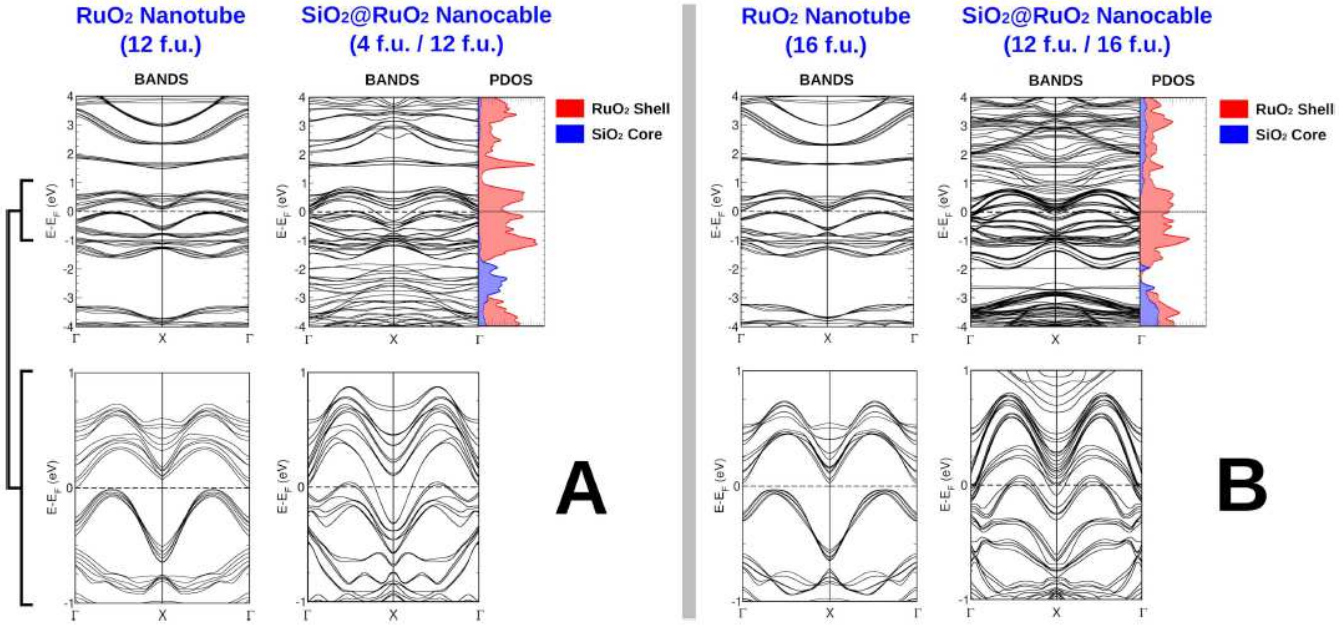

Figure 2. GW+BSE–corrected DFT band structure diagrams (referred to the Fermi energy) for the pure RuO_2 nanotubes with 12 and 16 functional units per unit cell (extracted from[10]), in comparison with those for the composite SiO_2@RuO_2 (4/12) and (12/16) nanowires, along the direction parallel to the nanotube axis. Two different views of the band diagram are given for each nanowire, displaying wide and narrow energy windows, respectively. Projected densities of states for the SiO_2 core and the RuO_2 shell are also included for the SiO_2@RuO_2 nanowires.

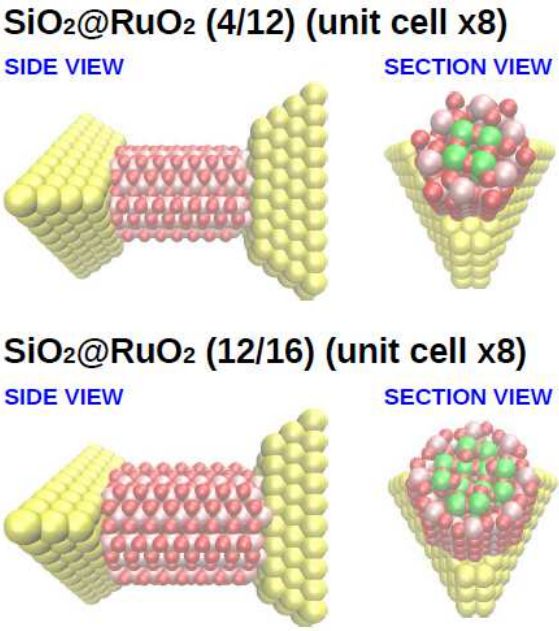

Figure 3. Side and section views of fragments of the SiO_2@RuO_2 (4/12) and (12/16) nanowires between gold electrodes with the shape of a truncated pyramid. The length of the nanowire fragments is eight times the unit cell. O, Si, Ru and Au atoms are represented by red, green, pink and yellow spheres, respectively.

We present first-principles calculations of the structural, electronic and transport properties of SiO_2@RuO_2 nanowires. Density functional theory (DFT) has been used to optimize the geometric structures of these wires. The electronic energy band structures of the nanowires have been improved by applying many-body techniques to account for self–energy corrections and excitonic effects. The RuO_2 shell has to adapt itself to the presence of the inner SiO_2 core, and this leads to important modifications in the electronic properties of the RuO_2 tube. Those modifications are a consequence of the structural changes in the outer shell of the nanocomposite as it adapts to the underlying core. The structural changes are small, but their effects on the electronic structure are strong. Electronic transport calculations have then been performed within the Fisher-Lee approach[17] by placing finite portions of the SiO_2@RuO_2 nanowires between two gold electrodes. In this way, we map electrical conductance versus energy, relating the transport properties with the electronic-structure. A promising result is the prediction of a drastic increase in the metallicity of the external RuO_2 shell and a sizable enhancement of the electronic transport, compared to the isolated RuO_2 nanotube. This occurs due to the presence of the core wire, which modifies the band structure of the external RuO_2 shell, thereby inducing multiple band-crossings with the Fermi level.

We have studied two SiO_2@RuO_2 nanowires with different diameters. The nanowires have been constructed from RuO_2 nanotubes and SiO_2 nanowires investigated in previous works.[10,16] The thin composite wire was formed from a SiO_2 nanowire with four SiO_2 units per cell confined inside a RuO_2 nanotube of twelve RuO_2 units per cell, and the thick wire was formed from a SiO_2 nanowire with twelve SiO_2 units per cell confined inside a RuO_2 nanotube of sixteen RuO_2 units per cell. In the following, these two composite nanowires will be called (4/12) and (12/16) nanowires, respectively. To optimize the structures, the starting geometries were thermally annealed by using a simulation method, which combines molecular dynamics (MD) and slow cooling quenching, implemented in FIREBALL (see[18] and references therein), a DFT code that uses a localized-basis set for the electronic wave functions. This

RSC Advances RSCPublishing

ARTICLE

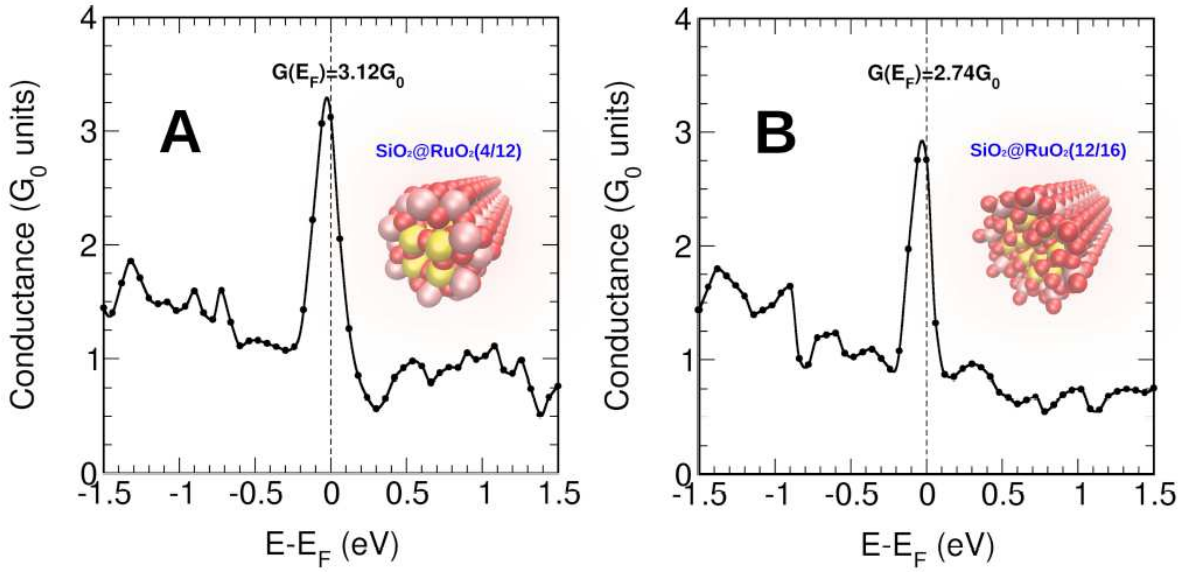

Figure 4. Calculated electrical conductance, in G_0 units, as a function of the energy, for the optimized SiO_2@RuO_2 (4/12) and (12/16) nanowire fragments of Figure 3 accommodated between gold electrodes (panels A and B, respectively).

technique has been successfully applied for obtaining global minimum energy structures of other one-dimensional-like systems[10,19] (further details in ESI). To improve the interaction between the core and shell parts of the composite wire, the structures obtained from the previous MD process were used as starting geometries in a steepest-descent reoptimization carried out with the plane-wave-based PWSCF code,[20] which implements a perturbative treatment of van der Waals interactions within the DFT+D approach[21] (see ESI). During the whole structural optimization process all atoms were allowed to relax, and the lattice parameter parallel to the nanowire axis was fully optimized. Additionally, in order to evaluate the robustness of the structures obtained, some tests were carried out by heating the system up to T=500K and the nanowires were found to be stable (full description in ESI).

Figure 1 shows the optimized SiO_2@RuO_2 (4/12) and (12/16) nanowire structures. The RuO_2 shell has to adapt to the presence of the inner SiO_2 core, and this results in a slight change of the average shell radius, which increases by 3% and 5% for the SiO_2@RuO_2 (4/12) and (12/16) wires, respectively, with respect to the starting RuO_2 nanotubes. A measure of the shell-core interaction can be obtained as $E_{int} = E(SiO_2@RuO_2) - [E(SiO_2) + E(RuO_2)]$. Here $E(SiO_2@RuO_2)$ is the total energy per unit cell of the composite nanowire; $E(SiO_2)$ and $E(RuO_2)$ are the energies of the SiO_2 core and RuO_2 shell fragments with exactly the same structure that these have in the composite wire. The values of the interaction energy per unit cell are -0.7 and -1.1 eV for the (4/12) and (12/16) nanowires. By noticing that the unit cells of those two nanowires have 48 and 84 atoms, respectively, those energies reveal a quite small interaction between core and shell. For this reason, SiO_2 appears to provide an efficient and quite inert scaffold to support the metal oxide shell. Nevertheless, the small dilatation of the interatomic distances in the shell RuO_2 compared to isolated RuO_2 wires leads to important modifications of the electronic band-structure.

The electronic band-structures for the optimized SiO_2@RuO_2 (4/12) and (12/16) nanowires have been obtained starting with the standard DFT electronic structure and applying many-body corrections by combining the quasi-particle GW approach[22,23] to account for the exchange-correlation self-energy, and the Bethe-Salpeter (BSE) equation[24,25] to account for excitonic effects (electron-hole interaction) in the unoccupied and excited states. For this purpose, the YAMBO simulation package[26] has been used (see details in ESI).

Figure 2 shows the GW+BSE–corrected DFT band structure diagrams (where E = 0 is taken at the Fermi energy). In that figure, the band structures parallel to the nanotube axis are compared to those for the pure isolated RuO_2 nanotubes in their own lowest energy equilibrium structure, along the high-symmetry line $\Gamma \rightarrow X \rightarrow \Gamma$. The bands of the two pure RuO_2 nanotubes (left columns in both A and B panels) exhibit a pronounced dispersion along this high-symmetry line. Those nanotubes behave as indirect gap semiconductors with gaps of nearly zero magnitude. On the other hand, the presence of the SiO_2 core induces substantial changes on the band structure of the RuO_2 shell. Focusing on the energy region between -1 eV and +1 eV around the Fermi level, a region dominated by RuO_2 states, there is a modest splitting of bands that were congested in pure RuO_2. A consequence is that the lowest unoccupied bands become stabilized and cross the Fermi level, and the highest occupied bands become destabilized and also cross the Fermi level. In this way, the composite SiO_2@RuO_2 nanowires develop multiple band-crossings with the Fermi energy (right

column in both A and B panels), drastically increasing their metallicity and conducting character. In the SiO_2@RuO_2 (4/12) nanowire, two previously occupied and two previously empty bands cross the Fermi level. The two previously occupied bands that now cross the Fermi level are degenerate in the proximity of the X point, and the same occurs with the two previously empty bands. This builds up a promising scenario for enhancing the conductance by the activation of new channels for electronic transport. Two of the crossing bands (those previously unoccupied) display a parabolic behavior in the crossing region, a signature of free-electron-like behavior, which increases substantially the mobility of the conduction electrons. Similarly, in the SiO_2@RuO_2 (12/16) nanowire, three previously occupied bands and one previously empty band cross the Fermi energy near the X point. As in the other composite wire, the previously empty band shows parabolic free-electron-like behavior in the crossing region. In addition, previously empty bands also cross the Fermi level at the Γ point.

It is interesting to point out that standard DFT calculations using the local density approximation (LDA) to exchange and correlation (that is, without many-body corrections) deliver band structures very similar to those in Figure 2, with the same main features and only minor specific differences. In particular, the enhancement of metallicity due to the bands crossing the Fermi level is also predicted (see ESI).

To understand better the origin of the mechanism underlying the drastic metallicity enhancement, we have calculated the GW+BSE-corrected DFT projected density of states (PDOS) onto the separate SiO_2 core and RuO_2 shell, for both SiO_2@RuO_2 (4/12) and (12/16) nanowires. The PDOS are shown also in Figure 2. The electronic bands in the region near the Fermi level come exclusively from the RuO_2 shell. The electronic states of the inner SiO_2 core play no role in the electronic conduction of the composite wires. The insulating SiO_2 core just acts as a scaffold to support the RuO_2 shell. However, it plays an indirect role in the enhancement of the metallicity of the RuO_2 shell by inducing a slight dilatation of the interatomic distances in the RuO_2 shell, and of the shell radius, which modifies the band structure of the external layer, yielding multiple band-crossings with the Fermi level.

The electronic transport properties of the SiO_2@RuO_2 nanowires have been investigated by using the Fisher-Lee Green-function method[17] (further details in ESI). For that purpose, we have relaxed portions of the SiO_2@RuO_2 nanowires between two gold electrodes. The electrodes have the form of truncated pyramids grown on gold surfaces. The nanowires had a length of eight unit cells, long enough to minimize the structural and electronic effects arising from the coupling with the electrodes, which could broaden the electronic levels of the nanotube. The optimized structures for the electrode/nanowire/electrode systems are shown in Figure 3. The conductance of the nanowires is plotted in Figure 4 as a function of electronic energy, for energies $E-E_F$ between -1.5 and 1.5 eV. The calculated conductance is given in G_0 units, where $G_0 = 2e^2/h$ is the quantum of conductance. A remarkable feature is the appearance of a high conductance peak at the Fermi energy for both wires. The peaks have values of 3.12 G_0 and 2.74 G_0 for the (4/12) and (12/16) nanowires, respectively, indicating high conductance through the nanowires when carriers are injected from the electrodes. Those prominent peaks, which arise from the bands crossing the Fermi level, do not appear when empty RuO_2 nanotubes are placed between the gold electrodes.[10] Comparison between the two panels of Figure 4 indicates that the influence of the wire diameter is low in this region of small diameters.

In addition, to address the influence of the wire length on the conductance pattern we have carried out calculations for a (4/12) SiO_2@RuO_2 nanowire fragment between the same two gold electrodes with a wire length of ten unit cells, to be compared with the results for a (4/12) SiO_2@RuO_2 nanowire fragment with a length of eight unit cells shown in Figure 4. The conclusion is that the conductance patterns of the two nanowire fragments – with nanotube lengths of eight and ten unit cells – are practically the same for the energy window between -1.5 and 1.5 eV, which guarantees converged results with respect to the nanowire length.

Consequently, the enhancement of the conductance has to be attributed to the presence of the inner SiO_2 core; that is, to the changes in the electronic band structure arising from the small elongation of the interatomic distances in the RuO_2 shell needed to accommodate to the core. Additional effects increasing the conductance may be the slight structural rearrangements of the nanowire fragments sandwiched between the Au electrodes, especially at the contact regions; and that, even in quasi-static equilibrium, electrons available from the Au electrodes redistribute the internal electronic charge of the nanowire (with the chemical potentials of electrodes and nanowire tending to align after the contacts are formed). Nevertheless, those effects are expected to be small compared to the main effect discovered here, that is, the changes in the band-structure of the nanotubes.

Conclusions

In summary, we have shown in this communication the reaches of the synergistic effect of core-shell SiO_2@RuO_2 nanowires. Such effect enhances significantly the metallic nature of the external RuO_2 shell, which in turn results in improved electronic conductance of the system. These highly conductive and stable core-shell nanostructures with reduced Ru-content open up the pathway for cost-effective applications in diverse fields such as nanoelectronics and electrocatalysis.

Acknowledgements

We acknowledge financial support from Spanish MINECO through Grants MAT2011-22781 and MAT2011-26534. JIM acknowledges the CSIC-JaeDoc fellowship programme, cofunded by the European Social Fund.

Notes and references

[a] Departamento de Superficies y Recubrimientos, Instituto de Ciencia de Materiales de Madrid (CSIC), ES-28049 Madrid, Spain.
[b] Université de Lyon, CNRS, École Normale Supérieure de Lyon, Laboratoire de Chimie, 46 Allée d'Italie, F-69364 Lyon Cedex 07, France.
[c] Institute of Theoretical Chemistry, Universität Stuttgart, D-70569 Stuttgart, Germany.
[d] Departamento de Física Teórica, Atómica y Óptica, Universidad de Valladolid, ES-47011 Valladolid, Spain.

*E-mail: joseignacio.martinez@icmm.csic.es

Electronic Supplementary Information (ESI) available: full calculation details: nanowire geometries and thermal-annealing molecular dynamics, many-body calculations, and Fisher-Lee transport formalism. See DOI: 10.1039/b000000x/

1 M. Grätzel, *Nature*, **2001**, *414*, 338.

2 G. M. Whitesides, and G. W. Crabtree, *Science*, **2007**, *315*, 796.

3 J. Hemminger, G. Crabtree, and M. Kastner, in *The Energy Challenges Report: New Science for a Secure and Sustainable Energy Future*, (Eds: J. Hemminger, G. Crabtree, and M. Kastner), Argonne National Laboratory: Argonne, IL, USA **2008**.

4 J. I. Martínez, H. A. Hansen, J. Rossmeisl, and J. K. Nørskov, *Phys. Rev. B*, **2009**, *79*, 045120.

5 Z. Bin, T. Tachikawa, P. Zhang, M. Fujitsuka, and T. Majima, *Nature Commun.*, **2014**, *5*, 3038.

6 E. J. W. Crossland, N. Noel, V. Sivaram, T. Leijtens, J. A. Alexander-Weber, and H. J. Snaith, *Nature*, **2013**, *495*, 215.

7 F. Hernandez-Ramirez, J. D. Prades, A. Hackner, T. Fischer, G. Mueller, S. Mathur, and J. R. Morante, *Nanoscale*, **2011**, *3*, 630.

8 D. Adler, *Rev. Mod. Phys.*, **1968**, *40*, 714.

9 D. J. Mowbray, J. I. Martínez, F. Calle-Vallejo, J. Rossmeisl, K. S. Thygesen, K. W. J. Jacobsen, and J. K. Nørskov, *J. Phys. Chem. C*, **2011**, *115*, 2244.

10 J. I. Martínez, E. Abad, F. Calle-Vallejo, C. M. Krowne, and J. A. Alonso, *Phys. Chem. Chem. Phys.*, **2013**, *15*, 14715.

11 S. Trasatti, *Electrochim. Acta*, **1991**, *36*, 225.

12 I. C. Man, H. Su, F. Calle-Vallejo, H. A. Hansen, J. I. Martínez, N. G. Inoglu, J. Kitchin, T. F. Jaramillo, J. K. Nørskov, and J. Rossmeisl, *ChemCatChem*, **2011**, *3*, 1159.

13 T. Kawai, and T. Sakata, *Chem. Phys. Lett.*, **1980**, *77*, 87.

14 V. Ozolins, F. Zhou, and M. Asta, *Acc. Chem. Res.*, **2013**, *46*, 1084.

15 C. N. Chervin, A. M. Lubers, K. A. Pettigrew, J. W. Long, M. A. Westgate, J. J. Fontanella, and D. R. Rolison, *Nano Lett.*, **2009**, *9*, 2316.

16 J. I. Martínez, F. Calle-Vallejo, C. M. Krowne, and J. A. Alonso, *J. Phys. Chem. C*, **2012**, *116*, 18973.

17 D. S. Fisher, and P. A. Lee, *Phys. Rev. Lett.*, **1981**, *23*, 6851.

18 J. P. Lewis, P. Jelínek, J. Ortega, A. A. Demkov, D. G. Trabada, B. Haycock, H. Wang, G. Adams, J. K. Tomfohr, E. Abad, H. Wang, and D. A. Drabold, *Phys. Stat. Sol. B*, **2011**, *248*, 1989.

19 E. Abad, C. González, J. I Martínez, F. Flores, and J. Ortega, *J. Nanopart. Res.*, **2014**, *16* 2262.

20 P. Giannozzi, *et al.*, *J. Phys.: Condens. Matter*, **2009**, *21*, 395502; URL: www.quantum-espresso.org.

21 S. Grimme, *J. Comp. Chem.*, **2006**, *27*, 1787.

22 M. S. Hybertsen, and S. G. Louie, *Phys. Rev. Lett.*, **1985**, *55*, 1418.

23 M. S. Hybertsen, and S. G. Louie, *Phys. Rev. B*, **1986**, *34*, 5390.

24 M. Rohlfing, and S. G. Louie, *Phys. Rev. Lett.*, **1999**, *83*, 856.

25 G. Onida, L. Reining, and A. Rubio, *Rev. Mod. Phys.*, **2002**, *74*, 601.

26 A. Marini, C. Hogan, M. Grüning, and D. Varsano, *Comput. Phys. Commun.*, **2009**, *180*, 1392.